

Influence of twin boundaries on Josephson junctions between high-temperature and conventional superconductors

M. Sigrist,* K. Kuboki,[†] and P. A. Lee

Department of Physics, Massachusetts Institute of Technology, Cambridge, Massachusetts 02139

A. J. Millis and T. M. Rice*

AT&T Bell Laboratories, Murray Hill, New Jersey 07974

(Received 5 May 1995; revised manuscript received 19 October 1995)

We give a consistent explanation of the c -axis Josephson tunneling experiment by Sun and co-workers between $\text{YBa}_2\text{Cu}_3\text{O}_{6+x}$ and Pb within the d -wave pairing scenario. Using a Ginzburg-Landau formulation, orthorhombic deformation and twinning of the crystal lattice are taken into account. In the presence of orthorhombic distortion, symmetry arguments allow a c -axis Josephson coupling between $\text{YBa}_2\text{Cu}_3\text{O}_{6+x}$ and Pb. However, for a highly twinned $\text{YBa}_2\text{Cu}_3\text{O}_{6+x}$ sample, the Josephson coupling is weakened due to destructive interference effects. On the other hand, we demonstrate that destructive effects due to twinning can be overcome, if twin boundaries support a state which locally breaks time reversal symmetry and leads to a channel which adds constructively to the total Josephson coupling. Properties of the Josephson junctions measured in experiment, such as the Fraunhofer pattern and the Fiske resonance, keep their standard form for such a junction. The existence of a twin boundary state with broken time reversal symmetry can directly be tested, for example, by observing vortices with fractional flux quanta on twin boundaries.

I. INTRODUCTION

The symmetry of the superconducting order parameter in CuO_2 systems has been hotly debated during recent years,¹ especially since generally microscopic theories predict a definite Cooper pairing symmetry. Leading candidates are various s -wave pairing states which are invariant under all crystal symmetry transformations and the so-called $d_{x^2-y^2}$ -wave state which is usually described by the generic pair wave function $\psi(\mathbf{k}) = \cos k_x - \cos k_y$.

Experiments have probed specific properties related to the symmetry, but, unfortunately, results seemingly in conflict with each other have led to considerable confusion. Various investigations of the quasiparticle excitation spectrum point towards the existence of zeros or nodes in the excitation gap. While this feature appears naturally for a d -wave superconductor due to the difference in sign of the wave function along the two main crystal axes, the gap of an s -wave state could have nodes too under certain conditions. One example of these experiments is that the low-temperature behavior of the London penetration depth in $\text{YBa}_2\text{Cu}_3\text{O}_{6+x}$ (YBCO) exhibits a temperature dependence which agrees strikingly well with predictions for a d -wave superconductor.² Furthermore, angle-resolved photoemission spectroscopy (ARPES) has revealed an angular dependence of the excitation gap for $\text{Bi}_2\text{SrCa}_2\text{Cu}_2\text{O}_8$ (BSCCO), which seem to be compatible with d -wave symmetry.^{3,4} However these experiments do not probe the pairing symmetry directly as they provide no access to the signs (or the phase) of the pair wave function in different momentum directions.

This deficiency was removed recently by a number of experiments based on the Josephson effect which is sensitive to the intrinsic phase structure of the order parameter. Many favor d -wave pairing. The sign change of the d -wave order

parameter under 90° rotation corresponds to a phase difference of π . This can lead to frustration effects in multiply connected superconductors and could be the origin of a peculiar paramagnetic signal seen in granular BSCCO (Wohllleben effect).^{5,6} The angular form of the pair wave function can be observed in a controlled way in an interferometer [superconducting quantum interference device (SQUID)] with a single crystal of YBCO and a conventional superconductor connected by two Josephson junctions. Several experiments done so far show indeed with improving accuracy such a phase difference π consistent with d -wave pairing symmetry.⁷ Other experiments make use of a loop with a phase twist of π , so that the flux quanta are half-integer multiples of the standard flux quantum $\Phi_0 (=hc/2e)$, $\Phi = \Phi_0(2n + 1)/2$, instead of $\Phi = n\Phi_0$. This new flux quantization has been observed recently and fits also well into the picture of a d -wave superconductor.⁸ Further support for d -wave symmetry comes from the modification of Fraunhofer interference patterns for weak Josephson junctions at a corner of a YBCO crystal.⁹

Nevertheless, these results have been challenged by two other experiments based on the idea of the probing Josephson couplings "forbidden" by symmetry. Chaudhari and Lin investigated the supercurrent flow out of a misoriented inclusion in a c -axis textured film of YBCO.¹⁰ The inclusion has a hexagonal shape with the crystal axes misaligned by 45° with respect to the surrounding. At first sight one would expect in this geometry that interference effects should cancel the total Josephson current if YBCO were a d -wave superconductor. Instead a finite current was measured. However, Millis showed that this can be understood, because the order parameter can realign itself to cancel the phase difference by introducing vortices of length scale λ_J (Josephson penetration depth).¹¹ The resulting magnetic fluxes at the interface

have recently been observed directly by scanning SQUID microscopy.¹²

In another experiment, Sun and co-workers demonstrated the existence of Josephson junctions in which a c -axis normal face of YBCO was coupled to superconducting Pb through a thin Ag layer (diffusion barrier).¹³ The quality of these superconducting-normal-superconducting (S - N - S) junctions was tested. The *Fraunhofer interference pattern* shows many oscillations of the critical current with applied magnetic field and the *Fiske resonances* appear with a very high Q factor.¹³ The product $I_c R$ of these junctions (the Josephson critical current times the normal state junction resistance) ranges from 0.05 to 2 mV depending on qualitative differences among the YBCO samples. These values are smaller than those estimated by Sun and co-workers based on the Ambegaokar-Baratoff theory.¹⁴

The existence of such high-quality junctions is difficult to understand, if YBCO is a d -wave superconductor. In a system with tetragonal crystal structure, symmetry would prevent any second (lowest) order Josephson coupling along the c axis to an s -wave superconductor such as Pb.¹⁵ Only higher order couplings (simultaneous coherent transmission of more than one Cooper pair) would contribute to the Josephson coupling, which are extremely small for tunneling junctions as used in these experiments. However, YBCO is orthorhombic; i.e., the a - and b axes of the basal plan are distinguished by length and by the presence of CuO chains parallel to the b axis. For this symmetry s and d waves cannot be distinguished anymore, but transform according to the same (trivial) irreducible representation. Thus, c -axis Josephson coupling would be allowed between a single crystal of YBCO and Pb. However, high-quality junctions were also made using highly twinned YBCO samples. These junctions are difficult to understand since we know that the d -wave order parameter of YBCO has different signs along the two main axes. This sign difference leads to a Josephson coupling along the c axis with opposite sign in neighboring twin domains, which would lead to a destructive interference and very weak macroscopic effects inconsistent with the experimental data.¹¹

In our view there are three possible explanations: (1) The order parameter in YBCO has basically s -wave symmetry and the previous experiments pointing towards a sign changes in the pair wave function were misinterpreted. (2) The Josephson coupling is not via the c axis, but instead comes from defects of the interface such as step edges which are induced because the orientation of the interface normal is not precisely along the c axis. (3) The twin boundaries yield an additional contribution to the Josephson coupling which produces the result observed by Sun and co-workers.¹³ In this paper we focus on the *third* possibility and its consequences.

We give here a brief outline of the basic ideas underlying our explanation. The orthorhombic lattice distortion $\epsilon = \epsilon_{xx} - \epsilon_{yy}$ introduces a natural coupling between the d -wave and an s -wave order parameter of the original tetragonal system, forming a *real* combination, a state we will call “ $d \pm s$ -wave” state [the relative phase of the two components is $0(+)$ or $\pi(-)$]. While the d -wave component does not couple to a standard (s -wave) superconductor along the c axis, the induced s -wave component leads to nonzero Jo-

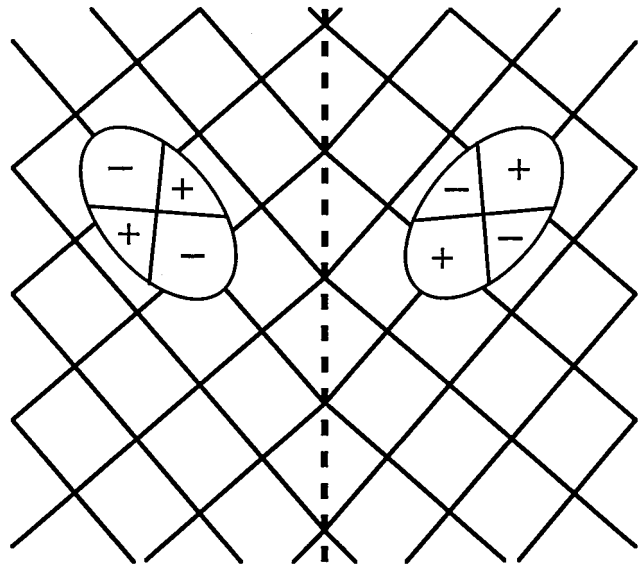


FIG. 1. Schematic structure of a twin boundary (dashed line) in an orthorhombically distorted crystal lattice. The ellipses denote the schematic structure of the pair wave functions on each side, which are a combination of s - and d -wave pairing. For the situation here the phase of the d -wave component is assumed to be constant while that of the s -wave component switches from 0 to π . This is the situation which will be discussed in this paper.

sephson tunneling. A complication occurs due to the formation of twin domains, characterized by either $\epsilon > 0$ or $\epsilon < 0$. They are separated by “domain walls,” so-called *twin boundaries* (TB’s) (see Fig. 1). In our approach the twin domains are also distinguished by the property that one type supports the $d + s$ - and the other the $d - s$ -wave state which leads to a sign change of the s -wave order parameter at each TB. Therefore, for a twinned YBCO sample the c -axis junction to an s -wave superconductor consists of an array of junctions with alternating sign of the Josephson coupling. Such an arrangement gives rise to destructive interference, which for random domain size leads to a reduction of the effective Josephson coupling by a factor proportional to $N^{-1/2}$ compared with that of an untwinned sample (N is the number of twin domains). In actual samples $N \sim 10^3 - 10^4$ and the Josephson penetration depth is larger than the linear extension of the interface.¹³ Therefore the argument given by Millis for the Chaudhari-Lin experiment does not apply here.¹¹ We cannot expect that nonuniform current flow could overcome the destructive interference effects. As the experiments on highly twinned YBCO do not show a drastic suppression of the Josephson effect, there must be a coupling channel which is not affected by this interference behavior.

A special superconducting state at the TB can provide such a channel. Naively we expect that at the TB the s -wave component changes sign by passing through zero. As a complex order parameter, however, it can avoid zero by going through the complex plane. This leads to a complex combination of s - and d -wave component, $d + e^{i\chi}s$ with $\chi \neq 0, \pi$. We will see in Sec. IV that such a state provides an additional Josephson coupling whose contributions can add constructively over all TB’s. This would yield a good, though inhomogeneous, Josephson junction. In Sec. V we demonstrate that the Fraunhofer interference pattern and the

Fiske modes behave as in homogeneous junctions in the experimentally tested samples. The properties of such an interface correspond to the averages over a large number of twin boundaries and inhomogeneity of the interface would not be visible. It is worth noting that this TB state breaks time reversal symmetry. This leads to unusual properties such as spontaneous currents or vortices with fractional flux quanta at the TB, which may be used for a direct test of the TB state (Sec. VI).

Note that our symmetry consideration leads to a different conclusion for BSCCO where the orthorhombic deformation of the crystal lattice is described by a shear strain $\epsilon = \epsilon_{xy}$, different from YBCO. This deformation does not yield a coupling between the s -wave and $d_{x^2-y^2}$ -wave order parameter, because in this case the two pairing states belong to different irreducible representations. Hence, by symmetry argument we would exclude Josephson coupling of BSCCO along the c axis to an s -wave superconductor. Indeed analogous experiments with a c -axis interface between BSCCO and an s -wave superconductor (Pb) have so far not shown any appreciable Josephson effect for junctions with a c -axis normal face.¹⁶

We adopt a phenomenological approach using a Ginzburg-Landau theory based on symmetry properties only. Consequently, the theory presented here can only account qualitatively for the effects we expect to occur in twinned YBCO.

II. GINZBURG-LANDAU THEORY OF A d - AND s -WAVE ORDER PARAMETER

In a system with tetragonal crystal field symmetry given by the point group D_{4h} the s -wave order parameter belongs to the trivial representation A_{1g} while the $d_{x^2-y^2}$ -wave order parameter transforms like the representation B_{1g} . Therefore their bare transition temperatures T_{cs} and T_{cd} are in general different. Purely based on symmetry arguments we can formulate the Ginzburg-Landau (GL) free energy functional which has to be a scalar under all possible symmetry transformations of D_{4h} , time reversal, and U(1) gauge symmetry. The free energy as an expansion in the two complex order parameters, $\eta_\mu = |\eta_\mu| \exp(i\phi_\mu)$ with $\mu = s$ for s wave and $\mu = d$ for d wave, is given by

$$\begin{aligned}
F[\eta_s, \eta_d, \mathbf{A}] = & \int d^3x \left[\sum_{\mu=s,d} \{ \tilde{a}_\mu(T) |\eta_\mu|^2 + b_\mu |\eta_\mu|^4 \right. \\
& + K_\mu |\mathbf{P}\eta_\mu|^2 \} + \gamma_1 |\eta_s|^2 |\eta_d|^2 + \frac{\gamma_2}{2} (\eta_s^{*2} \eta_d^2 \\
& + \eta_s^2 \eta_d^{*2}) + \frac{\tilde{K}}{2} \{ (P_x \eta_s)^* (P_x \eta_d) \\
& \left. - (P_y \eta_s)^* (P_y \eta_d) + \text{c.c.} \} + \frac{1}{8\pi} (\nabla \times \mathbf{A})^2 \right], \quad (1)
\end{aligned}$$

where $\tilde{a}_\mu(T) = a_\mu(T/T_{c\mu} - 1)$ and b_μ , K_μ , γ_1 , γ_2 , and \tilde{K} are real parameters. The vector \mathbf{P} denotes the gauge-invariant gradient $\nabla - (2\pi i/\Phi_0)\mathbf{A}$ (\mathbf{A} is the vector potential). Under

tetragonal symmetry no coupling of the two order parameters occurs at the level of second order expansion.^{17,18}

Let us consider the bulk properties of this free energy for $T_{cd} > T_{cs}$. Furthermore, we shall assume that $\gamma_1 > \gamma_2 > 0$. Naturally all the other parameters are positive, in particular $4b_s b_d > (\gamma_1 - \gamma_2)^2$, in order to guarantee the overall stability of the GL free energy. We find in general two distinct superconducting phases by lowering the temperature, a high-temperature phase with

$$\eta_{s0} = 0 \quad \text{and} \quad |\eta_{d0}|^2 = -\frac{\tilde{a}_d(T)}{2b_d}, \quad (2)$$

for $T_{cd} > T > T^*$, and a twofold degenerate low-temperature phase with

$$|\eta_{s0}|^2 = \frac{(\gamma_1 - \gamma_2)\tilde{a}_d - 2b_d\tilde{a}_s}{4b_s b_d - (\gamma_1 - \gamma_2)^2}, \quad (3)$$

$$|\eta_{d0}|^2 = \frac{(\gamma_1 - \gamma_2)\tilde{a}_s - 2b_s\tilde{a}_d}{4b_s b_d - (\gamma_1 - \gamma_2)^2},$$

for $T < T^*$ where the relative phase $\theta = \phi_s - \phi_d = \pm \pi/2$, because we took $\gamma_2 > 0$ ($\gamma_2 < 0$ would lead to $\theta = 0, \pi$). The lower transition point T^* is defined by the equation $(\gamma_1 - \gamma_2)\tilde{a}_d(T^*) = 2b_d\tilde{a}_s(T^*)$, i.e., $\eta_s(T^*) = 0$. By the choice of the parameters $\gamma_{1,2}$ the transition point T^* is lower than the bare transition temperature T_{cs} of η_s (in particular, there would be no transition if $T_{cs} \leq 0$). The low-temperature phase breaks time reversal symmetry \mathcal{T} because the time reversal operation acts on the order parameter by $\eta_\mu \rightarrow \eta_\mu^*$, relating θ to $-\theta$. We call this phase the $s \pm id$ state because $\theta = \pm \pi/2$.

Next we consider the effect of the orthorhombic distortion of the type $\epsilon = \epsilon_{xx} - \epsilon_{yy}$ as it is found in YBCO. We include this property in our theory only by adding the following term to the free energy functional:

$$F_\epsilon = c \epsilon \int d^3x (\eta_s^* \eta_d + \eta_s \eta_d^*), \quad (4)$$

where c is a real parameter which we choose to be positive. This term is the only scalar combination of the superconducting order parameters and ϵ under D_{4h} . There are two immediate consequences due to this new term: (1) The presence of a finite η_d forces also η_s to be finite (driven order parameter), and (2) the crystal lattice parameters are affected below the onset of superconductivity. Concerning the relative phase there is a competition between the fourth order term $\gamma_2(\eta_s^{*2} \eta_d^2 + \text{c.c.})$ and the second order term of F_ϵ . The former prefers $\theta = \pm \pi/2$ and the latter $\theta = 0$ or π . As long as both order parameters are small (close to T_{cd}) we expect that $\theta = 0$ (for $\epsilon < 0$) or π (for $\epsilon > 0$). At lower temperature a transition occurs when θ deviates continuously from these values, leading to a state with broken time reversal symmetry. Orthorhombic distortion suppresses the transition to the \mathcal{T} -violating state. Additionally, the coupling between the d - and s -wave order parameters in F_ϵ leads to a renormalization of the onset temperature of superconductivity,

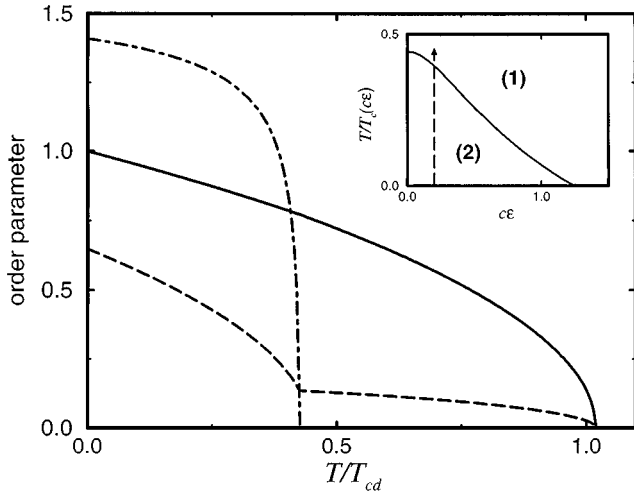


FIG. 2. Behavior of the order parameter as a function of temperature: $|\eta_d|$ (solid line), $|\eta_s|$ (dashed line) both in units of $|\eta_d(T=0)|$, and the relative phase $\theta = \phi_s - \phi_d$ (dot-dashed line). Inset: phase diagram with the \mathcal{F} -invariant (1) and the \mathcal{F} -violating (2) bulk phases. These results are obtained by solving the Ginzburg-Landau equations numerically for a generic choice of parameters: $a_{s,d}=1$, $b_{s,d}=0.5$, $K_{s,d}=1$, $\gamma_1=0.6$, $\gamma_2=0.5$, and $T_{cs}/T_{cd}=0.5$. For the plot of the order parameter we chose $c\epsilon=0.2$ (indicated in the inset by the dashed arrow).

$$T_c(c\epsilon) = \frac{T_{cd} + T_{cs}}{2} + \sqrt{\frac{(T_{cd} - T_{cs})^2}{4} + \frac{T_{cd}T_{cs}}{a_d a_s} (c\epsilon)^2}. \quad (5)$$

We neglect the change of volume, e.g., $\epsilon_{xx} + \epsilon_{yy}$, as another source to shift T_c , because it is not important at all for our discussion.

In Fig. 2 we show the behavior of the moduli of both order parameters and the relative phase as a function of temperature for a set of parameters in the GL free energy. The inset of Fig. 2 is the corresponding phase diagram, temperature versus $c\epsilon$, which shows clearly the suppression of the \mathcal{F} -violating phase due to the orthorhombic deformation. We remind the reader here that the results shown in these figures have only qualitative meaning, as the GL theory would be quantitatively valid only in the vicinity of the onset of superconductivity. In addition we have neglected here any change of ϵ with temperature.

The other interesting aspect is the influence of the coupling of the order parameters to ϵ in Eq. (4) on crystal lattice behavior. We replace ϵ by $\epsilon_0 + \delta\epsilon$, where ϵ_0 is the orthorhombic distortion just at the onset of superconductivity and $\delta\epsilon$ is a small deviation from this value. The elasticity energy for this small additional distortion is $F_{\text{elast}} = B\delta\epsilon^2/2$ where B is a (positive) elasticity constant of the lattice. Minimizing $F_{\text{elast}} + F_\epsilon$ with respect to $\delta\epsilon$ leads to

$$\delta\epsilon = -c(\eta_s^* \eta_d + \eta_s \eta_d^*)/B, \quad (6)$$

where the sign of $\delta\epsilon$ is the same as that of ϵ_0 , because F_ϵ is minimal if $\text{sgn}(\eta_s^* \eta_d + \eta_s \eta_d^*) = -\text{sgn}(\epsilon_0)$. Consequently, the presence of the superconducting phase enhances the orthorhombic deformation. This behavior is in qualitative agreement with experiments done with YBCO.^{19,20}

III. STATE NEAR A TWIN BOUNDARY

Orthorhombic deformation of a tetragonal lattice yields two degenerate crystal (twin) states characterized by $\epsilon > 0$ and $\epsilon < 0$. This allows the formation of so-called twin domains which are separated by twin boundaries (TB's) (see Fig. 1). We mentioned above that the relative phase between the two order parameters depends on the sign of ϵ so that a TB separates the state $d+s$ from $d-s$. It is reasonable to assume that at the TB the phase of one of the two order parameters changes from 0 to π , while the phase of the other would remain essentially constant. One can argue which of the two order parameter phases ϕ_s and ϕ_d would change in the case of YBCO. It is generally believed that the TB acts like a very good junction between the twin domains, which tends to keep the phase of the d -wave order parameter constant. On the other hand, the phase ϕ_d could be tied to the lattice deformation (for example, we could imagine that the CuO_2 chains in YBCO yield the dominant connection between the twin domains) such that it would change between 0 and π . In the following we assume the first case and η_s has to change the sign at the TB (as shown in Fig. 1). As will become clear below this assumption is equivalent to the argumentation by Sun and co-workers concerning the alternating phase (0 or π) of the Josephson coupling in an array of twin domains. We also emphasize that the other case would lead to a conflict in the interpretation of the SQUID and loop experiments mentioned above, where it is assumed that twinning does not affect the basal plane Josephson coupling along the main axes.^{7,8,21,22} Our assumption for the behavior of ϕ_d leads to a situation where the respective sign of the pair wave function along both main axis is the same in all twin domains.

Twin boundaries usually lie along the direction corresponding to [110] of the original tetragonal lattice (Fig. 1). Let us analyze the problem of a single TB located at $x-y=0$ which separates two half spaces. In this geometry the spatial variation of the order parameter occurs only along one dimension given by the coordinate $\tilde{x}=x-y$ while we can assume homogeneity along z and $\tilde{y} (=x+y)$ directions (x and y refer here always to the coordinates of the tetragonal system). The boundary conditions at infinity on the left and right hand sides of the TB corresponding to the bulk $d+s$ and $d-s$ states, respectively,

$$(\eta_d(\tilde{x}), \eta_s(\tilde{x})) = (\eta_{d0}, \pm \eta_{s0}) \text{ for } \tilde{x} \rightarrow \pm\infty, \quad (7)$$

where η_{d0} and η_{s0} are positive and real. The order parameter has two possibilities to connect the two domains: (I) $\eta_s(\tilde{x})/\eta_d(\tilde{x})$ is real every where, or (II) it becomes complex near the TB. Near the onset of superconductivity the second order term in F_ϵ dominates the behavior of the relative phase so that state (I) is realized. However, for lower temperature the fourth order (γ_2) term gains in importance and a continuous transition to state (II) happens. This instability can be understood by examining the structure of the GL theory. State (I) is described by a weakly \tilde{x} dependent $\eta_d(\tilde{x})$ ($\approx \eta_{d0}$) and $\eta_s(\tilde{x}) = \eta_{s0}f(\tilde{x})$ where $f(\tilde{x})$ is an odd function of \tilde{x} [$-1 \leq f(\tilde{x}) \leq +1$] which varies on a length scale

$$\xi(T) = \sqrt{K_s / [\tilde{a}_s(T) + 6b_s \eta_{s0}^2(T) + (\gamma_1 + \gamma_2) \eta_{d0}^2(T)]} \quad (8)$$

near the TB and $f(\tilde{x} \rightarrow \pm\infty) = \pm 1$. Both order parameter components are real. When does this state become unstable against a small admixture of imaginary components of the order parameter ($\eta_d(\tilde{x}) + iu(\tilde{x})$, $\eta_s(\tilde{x}) + iv(\tilde{x})$)? To answer this question we consider corrections of the GL free energy up to second order in u and v which has the structure

$$F_{uv} = \int d\tilde{x} d\tilde{y} [K_d(u')^2 + K_s(v')^2 + R_d u^2 + R_s v^2 + Quv], \quad (9)$$

with

$$\begin{aligned} R_d(\tilde{x}) &= \tilde{a}_d + 2b_d \eta_d^2(\tilde{x}) + (\gamma_1 - \gamma_2) \eta_s^2(\tilde{x}) \\ &= R_{d0} + (\gamma_1 - \gamma_2) V(\tilde{x}), \end{aligned}$$

$$R_s(\tilde{x}) = \tilde{a}_s + 2b_s \eta_s^2(\tilde{x}) + (\gamma_1 - \gamma_2) \eta_d^2(\tilde{x}) = R_{s0} + 2b_s V(\tilde{x}), \quad (10)$$

$$Q(\tilde{x}) = 4\gamma_2 \eta_s(\tilde{x}) \eta_d(\tilde{x}) + c\epsilon(\tilde{x}),$$

where $R_{d0} = R_d(\tilde{x} \rightarrow \infty)$ and $R_{s0} = R_s(\tilde{x} \rightarrow \infty)$. [Note that all first order terms in u and v vanish since $\eta_d(\tilde{x})$ and $\eta_s(\tilde{x})$ satisfy the GL equations.] The prime abbreviates the derivative with respect to \tilde{x} . The function $V(\tilde{x})$ denotes $\eta_{s0}^2(f(\tilde{x})^2 - 1) < 0$ and $Q(\tilde{x})$ is odd. (The stability of the homogeneous $s \pm d$ state implies the inequality $R_{d0}R_{s0} - Q_0^2 > 0$ [$Q_0 = |Q(\tilde{x} \rightarrow \pm\infty)|$]. The equality corresponds to the instability of this state against the \mathcal{T} -violating bulk phase discussed above.) We simplified our consideration here by neglecting the vector potential. Note that therefore the gradient term with the coefficient \tilde{K} in Eq. (1) does not appear here due to the symmetry of the coordinate \tilde{x} .²³

The variational equations to minimize F_{uv} are

$$K_d u'' = R_{d0} u + (\gamma_1 - \gamma_2) V(\tilde{x}) u + Q(\tilde{x}) v, \quad (11)$$

$$K_s v'' = R_{s0} v + 2b_s V(\tilde{x}) v + Q(\tilde{x}) u.$$

This linear differential equation system has only solutions for special values of the parameters (depending on the temperature T) which represent the instability conditions of state (I). The solution belonging to the largest temperature T determines the physical instability. This equation system has the form of a two-component Schrödinger equation with an attractive potential well, proportional to $V(\tilde{x})$, and a coupling $Q(\tilde{x})$ between the two components. Since $Q(\tilde{x})$ is an odd function, it follows that $u(\tilde{x})$ and $v(\tilde{x})$ have different parity under $\tilde{x} \rightarrow -\tilde{x}$. The physical instability corresponds to a bound state where both $u(\tilde{x})$ and $v(\tilde{x})$ are finite near the TB and decay exponentially for $\tilde{x} \rightarrow \pm\infty$ on a length scale $\tilde{\xi}$,

$$\tilde{\xi}^{-2} = r - \sqrt{r^2 - 4q^2}, \quad (12)$$

with $r = R_{s0}/K_s + R_{d0}/K_d$ and $q^2 = (R_{s0}R_{d0} - Q_0^2)/K_s K_d$. This length diverges as the bulk instability is approached ($q^2 \rightarrow 0$) and can therefore be rather long compared with ξ . In Appendix A we will show that the transition between states (I) and (II) occurs always at a temperature T' higher than the transition to the bulk \mathcal{T} -violating phase ($T' > T^*$).

The parity of u and v is essentially decided by the strength of the attractive potential for the two components. In

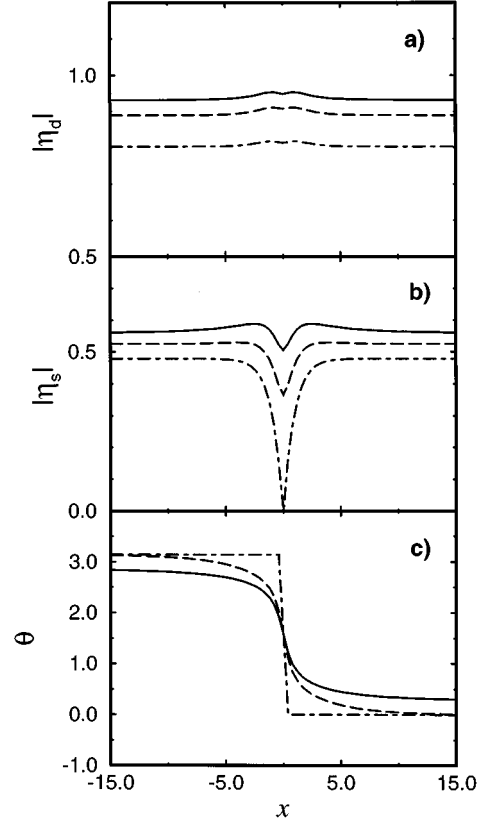


FIG. 3. Numerical solution for the twin boundary state at three different temperatures: For (a) $|\eta_d(\tilde{x})|$, (b) $|\eta_s(\tilde{x})|$, and (c) $\theta(\tilde{x})$ with the parameters in the Ginzburg-Landau theory as given in Fig. 2 with $c\epsilon = 1$. The temperatures are $T/T_{cd} = 0.1$ (solid line), 0.2 (dashed line), and 0.4 (dot-dashed line). They belong to the phases (2), (1,II), and (1,I) of Fig. 4, respectively.

the further discussion we shall assume that the instability leads to a state where $v(\tilde{x})$ is even, while $u(\tilde{x})$ is odd. For the relevant solution $v(\tilde{x})$ is nodeless and $u(\tilde{x})$ has just one node at $\tilde{x} = 0$. The resulting state is twofold degenerate because the (time reversal) transformation $(u, v) \rightarrow -(u, v)$ leads to another solution of the equations. Therefore, time reversal symmetry is broken locally at the TB by this state (II). In this state the relative phase $\theta(\tilde{x}) = \phi_s(\tilde{x}) - \phi_d(\tilde{x})$ changes in a smooth kink between 0 and π on the length $\tilde{\xi}$, in contrast to discontinuous jump for the state (I).

Unfortunately, analytic solution of the above equation system is difficult. (In Appendix A we will discuss the solution of a simplified version of these equations.) Therefore we analyzed the behavior of the order parameter in the vicinity of the TB by solving the complete GL equations numerically. In Fig. 3 we show the solutions for the parameters used in Fig. 2 and $c\epsilon = 1$ at three different temperatures. The highest temperature lies above T' such that TB state (I) is realized. The intermediate temperature show the locally \mathcal{T} -violating TB state (II), where the relative phase approaches 0 and π with a finite distance ($\tilde{\xi}$) from the TB. The lowest temperature is within the bulk \mathcal{T} -violating phase ($T < T^*$) and approaching the bulk the relative phase saturates at a value different from 0 or π .

We complete the phase diagram of the inset in Fig. 2 by adding the TB phase boundary line [$T'(c\epsilon)$]. The phase

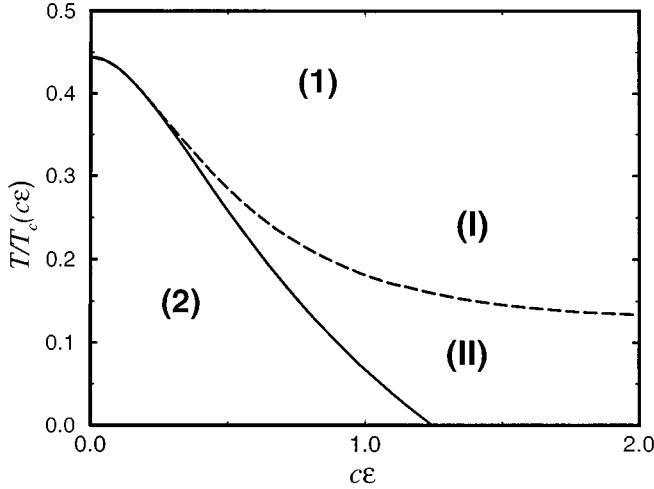


FIG. 4. Completed phase diagram including the twin boundary states (I) and (II). The parameters of the Ginzburg-Landau theory are chosen as in Fig. 2.

boundary merges naturally with the transition line [$T^*(c\epsilon)$] between the \mathcal{T} -invariant and \mathcal{T} -violating bulk phase for $c\epsilon \rightarrow 0$. In the limit $|c\epsilon| \gg a_d, a_s$, a simple scaling behavior (discussed in Appendix A) leads to $T(c\epsilon) \propto |c\epsilon|$. Note that $T'(c\epsilon)/T_c(c\epsilon) \rightarrow \text{const}$ in this limit. In Fig. 4 the phase diagram T versus $c\epsilon$ obtained numerically is shown.

Finally, we examine the problem of “interaction” between the degenerate \mathcal{T} -violating states on two TB’s lying close to each other. This problem can be considered within the instability equation [Eq. (10)] when two identical attractive potentials are included each at the position of one TB. The (fourfold) degeneracy of the bound states at the two TB’s is lifted by the formation of a bonding (even) or antibonding (odd) combination. (These states are still twofold degenerate because they break time reversal symmetry.) It is easy to see that the bonding configuration is favored and the “interaction energy” decreases exponentially with the distance $d \propto \exp(-d/\xi)$ (Appendix A). This configuration corresponds to a combination of kink and an antikink of $\theta(\tilde{x})$. In an array of TB’s this yields a sequence of alternating kinks and antikinks of $\theta(\tilde{x})$.

IV. PROPERTIES OF A JOSEPHSON JUNCTION

Following the goal of this article we discuss now the Josephson coupling at the interface between our superconductor $S1$ and a conventional s -wave superconductor $S2$ with the arrangement found in the experiment by Sun and co-workers; i.e., the interface between the two has a normal vector parallel to the c axis of the d -wave superconductor $S1$.¹³ The interface is assumed to have a square shape with a edge length L . As pointed out in the Introduction, the lowest order Josephson coupling via the d -wave order parameter η_d vanishes in this direction. The only contribution originates from the presence of η_s . Thus the local interface energy and the Josephson current are given by

$$\varepsilon_J = -\frac{I_0 \Phi_0}{2\pi c} |\eta_s| |\eta_0| \cos(\varphi - \theta),$$

$$J = I_0 |\eta_s| |\eta_0| \sin(\varphi - \theta) = I_c \sin(\varphi - \theta), \quad (13)$$

where $|\eta_s|$ and $|\eta_0|$ are the moduli of the s -wave order parameters at the interface on the side of $S1$ and $S2$, respectively. The phase difference between these two order parameters is denoted by φ . If the Josephson coupling is weak, then the order parameters should be affected only weakly by the presence of the interface. Therefore we assume that θ is the relative phase as given in the previous section. The superconductor $S1$ shall not be in the \mathcal{T} -violating bulk phase, but have state (II) on the TB.

Let us discuss the influence of the spatial variation of θ on φ by the standard sine-Gordon equation for Josephson junctions (\tilde{x} and \tilde{y} are the coordinates within the interface),

$$\left(\frac{\partial^2}{\partial \tilde{x}^2} + \frac{\partial^2}{\partial \tilde{y}^2} \right) \varphi = \lambda_J^{-2} \sin(\varphi - \theta), \quad (14)$$

with $\lambda_J = (\Phi_0/2\pi \tilde{d} I_c)^{1/2}$ the Josephson penetration depth, the length scale of variation of φ (\tilde{d} is the effective magnetic thickness, which is the sum of the London penetration depths of the two superconductors and the interface thickness).²⁴ It depends on the comparison of λ_J and the length scale of θ whether φ can follow the spatial variation of θ . If θ varies very rapidly over the length λ_J , then φ will adjust to an averaged modulation of θ only. The situation of interest for us corresponds exactly to this limit. In particular, in the following we will assume that $\lambda_J > L$ and the number of TB’s, N , is large so that the θ varies very rapidly.²⁷ This situation is different in the Chaudhari-Lin experiment¹⁰ where the length over which θ remains constant is the length of the hexagon edges which is much longer than λ_J .¹¹ In this case the phase difference φ can easily align itself with θ over most of the junction and compensate the effect of change of θ easily.

As we argued in the previous section neighboring TB’s favor alternating θ -kink and θ -antikink configurations. Although the energy difference for the kink-kink formation may be rather small, we will assume here that this alternation is realized. Thus, without loss of generality we can assume that θ varies between 0 and π via $\theta = \pi/2$ on each TB. We decompose $\cos(\varphi - \theta)$,

$$\cos(\varphi - \theta) = \cos\varphi \cos\theta + \sin\varphi \sin\theta, \quad (15)$$

where $\cos\theta$ changes sign in the range $0 \leq \theta \leq \pi$ and the contributions of neighboring twin domains ($\theta=0$ and $\theta=\pi$) tend to cancel each other. On the other hand, $\sin\theta$ is always positive and adds up constructively over all TB’s because θ changes between 0 and π for each TB through $\pi/2$ (or alternatively for each TB through $-\pi/2$) so that $\sin\theta$ has the same sign in each TB.

We consider now an array of parallel TB’s intersecting the interface. The position of the n th TB is given by $\tilde{x}_n - \tilde{x}_{n-1} = d + \zeta_n$. The deviations ζ_n of the distance between two TB’s from the average d are independent random variables with Gaussian distribution $\langle \zeta_n \rangle = 0$ and $\langle \zeta_n \zeta_{n'} \rangle = \sigma^2 \delta_{n,n'}$ ($\sigma < d$). Calculations are simplified if we consider the following approximate form of θ as a function of \tilde{x} :

$$\frac{2\theta(\tilde{x})}{\pi} = \begin{cases} 1 + (-1)^n \frac{(\tilde{x} - \tilde{x}_n)}{\tilde{\xi}}, & \tilde{x}_n \leq \tilde{x} \leq \tilde{x}_n + \tilde{x}', \\ 1 + (-1)^n, & \tilde{x}_n + \tilde{x}' \leq \tilde{x} \leq \tilde{x}_{n+1} - \tilde{x}', \\ 1 - (-1)^n \frac{(\tilde{x} - \tilde{x}_{n+1})}{\tilde{\xi}}, & \tilde{x}_{n+1} - \tilde{x}' \leq \tilde{x} \leq \tilde{x}_{n+1}, \end{cases} \quad (16)$$

where $\tilde{x}' = \tilde{\xi}$ if $\tilde{x}_{n+1} - \tilde{x}_n > 2\tilde{\xi}$ and $2\tilde{x}' = \tilde{x}_{n+1} - \tilde{x}_n$ if $\tilde{x}_{n+1} - \tilde{x}_n < 2\tilde{\xi}$. In the latter case the constant region of θ between \tilde{x}_n and \tilde{x}_{n+1} disappears. The extension $\tilde{\xi}$ of the regions with varying θ near the TB corresponds to the effective extension given in Eq. (12) and we use here the same symbol. Further, $I_c(\tilde{x})$ is not constant but shall have the value I_{c1} in regions where θ varies and I_{c2} where θ is constant.

For this form the interface energy per unit area is given by

$$\begin{aligned} \langle \varepsilon_J \rangle &= -\frac{\Phi_0}{2\pi c L^2} \int d\tilde{x} d\tilde{y} I_c(\tilde{x}) \cos[\varphi - \theta(\tilde{x})] \\ &= -\frac{\Phi_0}{2\pi c} (\langle I_c \sin\theta \rangle \sin\varphi + \langle I_c \cos\theta \rangle \cos\varphi), \end{aligned} \quad (17)$$

where $\langle \dots \rangle$ denotes the average over the random variables ζ_n . We consider first the average of $I_c \sin\theta$,

$$\langle I_c \sin\theta \rangle = \frac{4\tilde{\xi} I_{c1}}{\pi d} \left\langle \sin\left(\frac{\pi\tilde{x}'}{2\tilde{\xi}}\right) \right\rangle. \quad (18)$$

In the limit $d \gg \tilde{\xi}$ we find

$$\langle I_c \sin\theta \rangle \approx \frac{4\tilde{\xi} I_{c1}}{\pi d}, \quad (19)$$

which is proportional to the density $1/d$ of TB's, and for $d \ll \tilde{\xi}$,

$$\begin{aligned} \langle I_c \sin\theta \rangle &= \frac{4\tilde{\xi} I_{c1}}{\pi d} \left\langle \sin\left(\frac{\pi}{4\tilde{\xi}}(d + \zeta)\right) \right\rangle \approx I_{c1} \left\langle \cos\left(\frac{\pi\zeta}{4\tilde{\xi}}\right) \right\rangle \\ &\approx I_{c1} \left[1 - \frac{\pi^2 \sigma^2}{32\tilde{\xi}^2} \right], \end{aligned} \quad (20)$$

where we keep in mind that $\sigma < d$. Note that I_{c1} is proportional to $|\eta_s|$ in the TB which would also depend on the density of TB's too. Therefore in the limit $d \ll \tilde{\xi}$ we would expect that I_{c1} would be reduced due to the suppressive effect of the TB on the s -wave order parameter (change of sign or phase).

For the average of $I_c \cos\theta$ we have to take into account that neighboring domains contribute with opposite sign and tend to cancel each other,

$$\begin{aligned} \langle I_c \cos\theta \rangle &= \left\langle \int_{\tilde{x}_n}^{\tilde{x}_{n+1}} d\tilde{x} I_c(\tilde{x}) \cos\theta(\tilde{x}) \right\rangle \\ &= \left\langle (-1)^n \left[I_{c2}(\tilde{x}_{n+1} - \tilde{x}_n - 2\tilde{x}') \right. \right. \\ &\quad \left. \left. - \frac{2\tilde{\xi} I_{c1}}{\pi} \cos\left(\frac{\pi\tilde{x}'}{2\tilde{\xi}}\right) \right] \right\rangle, \end{aligned} \quad (21)$$

which for $d \gg \tilde{\xi}$ is

$$\begin{aligned} \langle I_c \cos\theta \rangle &= \frac{I_{c2}}{Nd} \left\langle \sum_{n=1}^{N/2} (\zeta_{2n-1} - \zeta_{2n}) \right\rangle \\ &= \frac{I_{c2}}{Nd} \left[\sum_{n=1}^{N/2} \langle (\zeta - \zeta')^2 \rangle \right]^{1/2} = \frac{\sigma I_{c2}}{d\sqrt{N}} \end{aligned} \quad (22)$$

and for $d \ll \tilde{\xi}$ is

$$\begin{aligned} \langle I_c \cos\theta \rangle &= \frac{I_{c1}}{2Nd} \left\langle \sum_{n=1}^N (-1)^n \cos\left(\frac{\pi}{4\tilde{\xi}}(d + \zeta_n)\right) \right\rangle \\ &\approx \frac{\pi I_{c1}}{2\tilde{\xi} N} \left[\sum_{n=1}^{N/2} \langle (\zeta - \zeta')^2 \rangle \right]^{1/2} = \frac{\pi \sigma I_{c1}}{\tilde{\xi} \sqrt{N}}. \end{aligned} \quad (23)$$

In both cases the central limit theorem leads to $N^{-1/2}$ dependence.

The Josephson current phase relation can be obtained by the derivative of the interface energy with respect to φ ,

$$J = \frac{2\pi c}{\Phi_0} \frac{d\langle \varepsilon_J \rangle}{d\varphi} = \langle I_c \sin\theta \rangle \cos\varphi - \langle I_c \cos\theta \rangle \sin\varphi, \quad (24)$$

and the maximum current is immediately obtained as

$$J_{\max} = \sqrt{\langle I_c \sin\theta \rangle^2 + \langle I_c \cos\theta \rangle^2}. \quad (25)$$

The phase φ which minimizes the interface energy corresponds to $J(\varphi_0) = 0$,

$$\tan\varphi_0 = \frac{\langle I_c \sin\theta \rangle}{\langle I_c \cos\theta \rangle}, \quad (26)$$

and the phase shift φ_0 approaches $\pi/2$ for $N \gg 1$. Obviously, the contributions due to the TB state dominate the Josephson effect in case of large N . For $\tilde{\xi} < d$ the coupling should increase essentially proportionally to the density of TB's, $J_{\max} \approx 4\tilde{\xi}I_{c1}/\pi d$. It reaches a maximum for $\tilde{\xi} \sim d$ and decreases for increasing density of TB's ($\tilde{\xi} > d$) again, because I_{c1} and I_{c2} become gradually smaller. [Note that even in state (II) the TB suppresses the s -wave order parameter locally.] In the experiment by Sun and co-workers the average distance between TB's is of the order $d \sim 10^2 - 10^3$ Å. As we mentioned in Sec. III it is possible that $\tilde{\xi}$ can be rather large although ξ is very short. Therefore it is not unrealistic to assume that $\tilde{\xi}$ could be of the same order of magnitude as d . However, our qualitative considerations do not allow to give any reliable estimate of $\tilde{\xi}$.

V. PROPERTIES OF THE INTERFACE IN A WEAK MAGNETIC FIELD

In this section we consider phenomena in connection with a magnetic field parallel to the interface. The phase difference φ at the junction obeys the equation

$$\left(\frac{\partial}{\partial \tilde{x}}, \frac{\partial}{\partial \tilde{y}} \right) \varphi = \frac{2\pi\tilde{d}}{\Phi_0} (B_{\tilde{y}}, -B_{\tilde{x}}) = (k_{\tilde{x}}, k_{\tilde{y}}), \quad (27)$$

with \tilde{d} the effective magnetic width of the interface. For very weak Josephson coupling such that λ_j is much larger than L , the magnetic field spreads uniformly throughout the interface. Then the local phase difference $\varphi(\tilde{\mathbf{r}})$ is

$$\varphi(\tilde{\mathbf{x}}) = \alpha + \mathbf{k} \cdot \tilde{\mathbf{r}}, \quad (28)$$

with $\tilde{\mathbf{r}} = (\tilde{x}, \tilde{y})$. Obviously, \mathbf{k} corresponds to the inverse lengths $\ell_{\tilde{x}} = 2\pi/k_{\tilde{x}}$ and $\ell_{\tilde{y}} = 2\pi/k_{\tilde{y}}$, which define the extension of one flux quantum Φ_0 within the interface.

The phase modulation due to the magnetic field leads to interference effects (Fraunhofer pattern) and in combination with a voltage on the junction to (Fiske) resonance phenomena. We discuss here whether the inhomogeneity of the interface would modify these properties. For simplicity we will assume that the (square) interface edges are parallel to the \tilde{x} and \tilde{y} axes, respectively, and the TB's are again parallel to the \tilde{x} axis.

A. Fraunhofer pattern

We study first the interference effects observable in the total Josephson current given by

$$I_{\text{tot}} = \int_{-L/2}^{L/2} d\tilde{x} \int_{-L/2}^{L/2} d\tilde{y} I_c(\tilde{x}) \sin[\alpha - \theta(\tilde{x}) + \mathbf{k} \cdot \tilde{\mathbf{r}}], \quad (29)$$

which after integration over \tilde{y} leads immediately to

$$I_{\text{tot}} = L \frac{\sin(k_{\tilde{y}}L/2)}{k_{\tilde{y}}L/2} \int_{-L/2}^{L/2} d\tilde{x} I_c(\tilde{x}) \sin[\alpha - \theta(\tilde{x}) + k_{\tilde{x}}\tilde{x}]. \quad (30)$$

If the field lies perpendicular to the TB, $k_{\tilde{x}} = 0$, then the inhomogeneity of the interface does not affect the interference effect at all and the total current maximized with respect to α is given by the standard form

$$I(\Phi) = J_{\max} L^2 \left| F\left(\frac{\pi\Phi}{\Phi_0}\right) \right|, \quad (31)$$

with J_{\max} from Eq. (25), $F(x) = \sin(x)/x$ and $\Phi = |k_{\tilde{y}}L/2\pi| = |\tilde{d}LB_{\tilde{x}}|$ as the total flux threading the interface.

On the other hand, if the magnetic field is parallel to the TB, the maximal current has the form

$$I(\Phi) = L^2 \left[\left\langle I_c \sin\theta \right\rangle F\left(\frac{\pi\Phi}{\Phi_0}\right) \right]^2 + \left\langle I_c \cos\theta \right\rangle^2 F\left(\frac{2\pi\Phi}{\Phi_0}\right) \right]^{1/2}, \quad (32)$$

which in the large- N limit is dominated by the first term,

$$I(\Phi) = \langle I_c \sin\theta \rangle L^2 \left| F\left(\frac{\pi\Phi}{\Phi_0}\right) \right| + O(N^{-1}) \quad (33)$$

(for details see Appendix B). Up to small corrections the maximal current follows the standard Fraunhofer interference pattern and the effects of the inhomogeneity of the interface are not observable.

B. Fiske resonance

The interface can also act as a wave guide supporting discrete modes of electromagnetic waves with a definite momentum-frequency relation $\omega = vk$ where $v = c/\sqrt{\tilde{d}C}$ with C as the capacitance of the interface per unit area and c as the speed of light. By applying a voltage V and a magnetic field B such modes can be excited. In particular these modes appear in form of resonances in the dc Josephson current. We follow here the standard method for analyzing this problem.²⁵ For a very weak junction the phase difference φ is a function of position and time,

$$\varphi(\tilde{x}, t) = \omega t - \mathbf{k} \cdot \tilde{\mathbf{r}} + \alpha + \tilde{\varphi}(\tilde{x}, t), \quad (34)$$

where $\omega = 2\pi V/\Phi_0$ and the function $\tilde{\varphi}(\tilde{\mathbf{x}}, t)$ is a small correction to the other terms. The sine-Gordon equation [Eq. (14)] has to be extended to describe also the time dependence of the phase and dissipation effects,

$$\left(\frac{\partial^2}{\partial \tilde{\mathbf{r}}^2} - \frac{1}{v^2} \frac{\partial^2}{\partial t^2} - \Gamma \frac{\partial}{\partial t} \right) \varphi = \lambda_j^{-2} \sin[\varphi - \theta(\tilde{x})], \quad (35)$$

with Γ as the dissipation rate.²⁵ In the large- N limit this equation reduces to

$$\left(\frac{\partial^2}{\partial \tilde{\mathbf{r}}^2} - \frac{1}{v^2} \frac{\partial^2}{\partial t^2} - \Gamma \frac{\partial}{\partial t} \right) \tilde{\varphi} = \frac{2\pi\tilde{d}}{\Phi_0} \text{Im} \langle I_c e^{-i\theta} \rangle e^{i(\omega t - \mathbf{k} \cdot \tilde{\mathbf{r}} + \alpha)} \quad (36)$$

(see Appendix B). This equation can be solved immediately,

$$\tilde{\varphi}(\tilde{\mathbf{x}}, t) = \frac{2\pi\tilde{d}}{\Phi_0} \text{Im} \frac{\langle I_c e^{-i\theta} \rangle}{(\omega^2/v^2 - k^2) - i\Gamma\omega} e^{i(\omega t - \mathbf{k} \cdot \tilde{\mathbf{r}} + \alpha)}. \quad (37)$$

Inserting this result into φ of Eq. (34) we find the dc current

$$J_{\text{dc}} = \frac{\Gamma \omega}{(\omega^2/v^2 - k^2)^2 + \Gamma^2 \omega^2} \frac{\pi \tilde{d}}{\Phi_0} J_{\text{max}}^2, \quad (38)$$

as shown in Appendix B. As in the standard case the dc current shows a resonance if the voltage and the magnetic field match the condition $\omega = vk$.

Both the Fraunhofer interference pattern and the Fiske resonance are not modified qualitatively compared with the behavior of usual junctions, if N is very large (highly twinned sample). This is only true as long as the applied field is sufficiently small, in the sense that the length $\ell \sim 1/k_{\tilde{x}}$ is much larger than the average distance d between the TB's. In a measurement of the total current we observe only the properties averaged over a large number of twin domains. The varying $\theta(\tilde{x})$ introduces phase modulations with many wave vectors $\mathbf{q} [= (q_{\tilde{x}}, 0)]$ which lead to dominant contributions for $q_{\tilde{x}} = \pi n/d$ (see Appendix B). However, very large fields ($k_{\tilde{x}} \sim \pi/d$) were necessary to reveal the inhomogeneous structure of the interface by examining interference effects. Such magnetic fields correspond to a flux of the order $N\Phi_0$ in the interface. We cannot expect that a Josephson tunneling junction would still work under such conditions.

VI. OTHER EXPERIMENTAL CONSEQUENCES

We consider now properties of the system which could be used to test some aspects of the picture developed here. The first probe is connected with the average phase shift φ_0 which for the highly twinned samples approaches $\pi/2$. The two next effects are based on specific magnetic properties of the \mathcal{T} -violating state. Finally we consider also the presence of soft modes due to the phase transition from state (I) to (II).

A. Average phase shift φ_0

For the c -axis interface between the s wave and a highly twinned sample of YBCO the Josephson current-phase relation is given by

$$J = J_{\text{max}} \sin(\varphi - \varphi_0), \quad (39)$$

where J_{max} and φ_0 are defined in Eqs. (25) and (26), respectively. We can arrange the geometry of the s -wave superconductor so that it forms a second junction with the YBCO sample, this time along the basal plane direction of YBCO (basal plane junction with the critical current I_c). In this way we create a superconducting loop where the latter junction is in general much stronger than the c -axis junction discussed above. Due to the phase shift φ_0 we expect that the order parameter phase around the loop is twisted. This can lead to a spontaneous current and a magnetic flux through the loop. The fact that the c -axis junction is weak, however, leads to the problem that the flux is not well quantized and, in particular, not in a simple topological way related to φ_0 .

Let us analyze the behavior of the current in such a loop, assuming that the basal plane contact is much stronger than the one along c axis, i.e., the dimensionless parameter $2\pi LI_c/\Phi_0 c \gg 1$ (L is the self-inductance of the loop). On the other hand, the analogous parameter shall be much smaller than 1 for the c -axis junction ($\gamma = 2\pi LJ_{\text{max}}/\Phi_0 c \ll 1$). In this case currents flowing in the loop are so small that the current-phase relation of basal plane junction can be

approached by $I = I_c \sin \varphi \approx I_c \varphi$. Therefore we can write an energy expression as a function of the current in the loop containing the contribution of the c -axis junction only and the magnetic field energy ($\propto I^2$),

$$E(I) = \frac{1}{2c^2} LI^2 - \frac{\Phi_0 J_{\text{max}}}{2\pi c} \cos\left(\frac{2\pi LI}{\Phi_0 c} - \varphi_0\right). \quad (40)$$

Minimizing this energy with respect to I we obtain the flux

$$\Phi = \frac{1}{c} LI = \frac{1}{c} LJ_{\text{max}} \sin \varphi_0 + O(\gamma^2), \quad (41)$$

which is finite only if φ_0 is different from 0 and π . Hence, according to our picture the c -axis junction of a highly twinned sample would lead to finite flux, while in contrast no flux would be expected in the case YBCO were a pure s -wave superconductor or the sample were untwinned ($\varphi_0 = 0$ or π).

B. Spontaneous currents in the twin boundary

It is known for some time that in \mathcal{T} -violating superconductors domain walls can carry supercurrents even in the absence of external fields.^{17,28} These spontaneous currents flow parallel to the domain walls and generate a local magnetic field distribution. No net magnetization is resulting from these currents, because screening effects lead to an overall canceling of the fields. Such currents flow also in TB's with a \mathcal{T} -violating state. We will illustrate this here briefly by examining the structure of the supercurrent in the basal plane, $J_\alpha = -c \partial F / \partial A_\alpha$ where F is given in Eq. (1) ($\alpha = x, y$),

$$\begin{aligned} J_\alpha = \frac{2\pi c}{\Phi_0} & \left[\sum_{\mu=s,d} K_\mu |\eta_\mu|^2 \left(\frac{\partial}{\partial \alpha} \phi_\mu - \frac{2\pi}{\Phi_0} A_\alpha \right) \right. \\ & + \tilde{K} s_\alpha \left(\left| \eta_s \right| \frac{\partial}{\partial \alpha} |\eta_d| - \left| \eta_d \right| \frac{\partial}{\partial \alpha} |\eta_s| \right) \sin \theta \\ & \left. + \left(\frac{\partial}{\partial \alpha} (\phi_s + \phi_d) - \frac{4\pi}{\Phi_0} A_\alpha \right) |\eta_s| |\eta_d| \cos \theta \right], \quad (42) \end{aligned}$$

with $\eta_\mu = |\eta_\mu| \exp(i\phi_\mu)$, $\theta = \phi_s - \phi_d$, and $s_x = +1$ and $s_y = -1$. Far away from the surface of the sample we find that the current perpendicular to the TB (J_\perp) has to vanish in any case due to Meissner screening effects described by the London equation $\nabla \times \mathbf{B} = 4\pi \mathbf{J}/c$. In the analysis of this equation it is important to notice that deep inside the sample the only spatial dependence is along the normal vector $\mathbf{n} [= (1, 1, 0)]$ of the TB. Thus,

$$\begin{aligned} 0 = J_\perp = \mathbf{n} \cdot \mathbf{J} = J_x + J_y = \frac{4\pi c}{\Phi_0} & \left[\sum_{\mu=s,d} K_\mu |\eta_\mu|^2 \left(\frac{\partial \Phi_\mu}{\partial \tilde{x}} \right. \right. \\ & \left. \left. - \frac{2\pi}{\Phi_0} A_{\tilde{x}} \right) + \frac{4\pi}{\Phi_0} \tilde{K} |\eta_s| |\eta_d| A_{\tilde{y}} \cos \theta \right], \quad (43) \end{aligned}$$

with $A_{\tilde{x}} = A_x + A_y$ and $A_{\tilde{y}} = A_x - A_y$. The current parallel to the TB is given by

$$J_{\parallel} = J_x - J_y = \frac{4\pi c}{\Phi_0} \tilde{K} \left[\left\{ |\eta_s| \frac{\partial}{\partial \tilde{x}} |\eta_d| - |\eta_d| \frac{\partial}{\partial \tilde{x}} |\eta_s| \right\} \sin\theta \right. \\ \left. + \left\{ \frac{\partial}{\partial \tilde{x}} (\phi_s + \phi_d) - \frac{4\pi}{\Phi_0} A_{\tilde{x}} \right\} |\eta_s| |\eta_d| \cos\theta \right]. \quad (44)$$

The structure of the \mathcal{T} -violating state leads to $\sin\theta$ and $|\eta_{\mu}|$ that are even functions of \tilde{x} with respect to the center of the TB ($\tilde{x}=0$), while $\cos\theta$ is an odd function. Combining Eqs. (43) and (44) it is easy to see that J_{\parallel} is nonzero and an odd function; i.e., the supercurrent flows in opposite directions on the two sides of the TB. This current distribution generates a magnetic field pointing along the z direction which is peaked in the center of the TB. It changes sign and approaches gradually zero on a length of the London penetration depth further away from the TB due to screening effects.²⁹

A very rough estimate of the magnitude of the field in the center of the TB can be obtained by neglecting screening effects and the spatial dependence of the moduli of the order parameter $|\eta_{\mu}|$. Then θ is the only \tilde{x} -dependent quantity changing continuously from 0 to π at the TB. Using Eqs. (43) and (44) within this approach we obtain the equation

$$\frac{\partial B_z}{\partial \tilde{x}} = \frac{8\pi^2}{\Phi_0} \tilde{K} |\eta_s| |\eta_d| \left\{ \frac{K_d |\eta_d|^2}{K_d |\eta_d|^2 + K_s |\eta_s|^2} \right\} \cos\theta \frac{\partial \theta}{\partial \tilde{x}}, \quad (45)$$

where we set $\mathbf{A}=0$ in the current expressions. The magnetic field at $\tilde{x}=0$ is obtained by simple integration with respect to \tilde{x} ,

$$B_z(\tilde{x}=0) = 2 \left(\frac{2\pi}{\Phi_0} \right)^2 \tilde{K} |\eta_s| |\eta_d| \left\{ \frac{K_d |\eta_d|^2}{K_d |\eta_d|^2 + K_s |\eta_s|^2} \right\} \Phi_0, \quad (46)$$

with $\sin\theta(\tilde{x}=0)=1$. We can estimate this expression by considering the anisotropy of the London penetration depth,

$$\frac{1}{4\pi\lambda_{\alpha}^2} = 2 \left(\frac{2\pi}{\Phi_0} \right)^2 [K_s |\eta_s|^2 + K_d |\eta_d|^2 + \tilde{K}_{S\alpha} |\eta_s| |\eta_d| \cos\theta], \quad (47)$$

which leads to

$$2 \left(\frac{2\pi}{\Phi_0} \right)^2 \tilde{K} |\eta_s| |\eta_d| = \frac{1}{8\pi} |\lambda_x^{-2} - \lambda_y^{-2}|. \quad (48)$$

Furthermore, the ratio in $\{\dots\}$ may lie somewhere between 0.1 and 1. Thus, we find

$$B_z(0) \sim (0.1-1) \frac{\Phi_0}{8\pi} |\lambda_x^{-2} - \lambda_y^{-2}|. \quad (49)$$

If we assume that this formula gives a reasonable estimate also at low temperatures (where the GL theory is not exact anymore), we may use the zero temperature values of the London penetration depth ($\lambda \approx 1600$ and 1000 Å). This leads to $B_z(0) \sim 5-50$ G. This estimate is surely too high. Screening effects and reduction of the order parameter close to the TB would reduce this value. Even if these effects would diminish the estimated field by one or two orders of

magnitude, it still could be observable. Unfortunately, the internal variation of the field occurs on a length of ξ , so that the magnetization would have canceled to zero on the scale of London penetration depth. Therefore, this is not a favorable condition to do any kind of magnetic microscopy searching for these fields. In addition it is not so clear how sensitive the TB states are to the conditions at the surface. A technique more likely to reveal the presence of such a spontaneous current and field distribution is μ SR (muon spin rotation) in zero external field. When (spin polarized) muons are injected into a sample, they are trapped at specific crystallographic positions throughout the volume. The measurement of their dipolarization rate provides a good probe for the local magnetic field at the trapping points. As they sample the local field over the whole volume of the sample they can give information of the overall field distribution. Hence, it is possible to observe the change in the internal field distribution below the transition to the \mathcal{T} -violating TB state. We would like to emphasize that in a similar way such signals have demonstrated the occurrence of internal magnetic fields for superconducting phases which break time reversal symmetry in the heavy fermion compounds UPt_3 and $\text{U}_{1-x}\text{Th}_x\text{Be}_{13}$.

C. Fractional vortices on twin boundaries

For well-separated TB's the \mathcal{T} -violating state is twofold degenerate. Therefore both degenerate states may appear as domains on the TB's separated by boundary lines, similar to Bloch lines in the domain walls of ferromagnets. These boundary lines correspond to the phase winding of the s -wave order parameter and carry a topological charge, i.e., a magnetic flux (see Ref. 30). The magnetic flux enclosed in this line is, in general, only a fraction of Φ_0 . This can be understood in the following way. Consider an isolated domain boundary line, where on one side θ passes through $+\pi/2$ and on the other side through $-\pi/2$ in the TB. We encircle the line with a path sufficiently far that it contains all the flux associated with the line. The path has rectangular shape with two edges a and a' perpendicular to the TB, while the other two edges b and b' lie parallel to the TB. All path segments are located so that there is no current flowing parallel to them: $J_{\perp}=0$ on a and a' and $J_{\parallel}=0$ on b and b' . Using Eqs. (43) and (44) it is easy to arrive at the integral

$$\oint_{a,b,a',b'} d\mathbf{s} \cdot \left(\nabla \phi - \frac{2\pi}{\Phi_0} \mathbf{A} \right) \\ = \left(\int_a d\tilde{x} - \int_{a'} d\tilde{x} \right) \left[\frac{K_s |\eta_s|^2}{K_s |\eta_s|^2 + K_d |\eta_d|^2} \frac{\partial \theta}{\partial \tilde{x}} \right. \\ \left. + \frac{4\pi}{\Phi_0} \frac{\tilde{K} |\eta_s| |\eta_d| A_{\tilde{y}} \cos\theta}{K_s |\eta_s|^2 + K_d |\eta_d|^2} \right], \quad (50)$$

where we introduced $\phi_d = \phi$ and $\phi_s = \phi + \theta$. Note that the integrals on b and b' do not contribute to the right hand side, because these segments are taken very far from the TB. The first integrand on the right hand side of Eq. (50) gives obviously a fraction of 2π depending on the system parameters like K_s and K_d . This is true also for the second integrand, because $A_{\tilde{y}}$ is generated by the currents running along the TB

(J_{\parallel}) so that its contribution is roughly proportional to $(\tilde{K}|\eta_s||\eta_d|)^2$. Note that the integrands are identical in magnitude on a and a' and however, have opposite sign. We obtain for the flux Φ from Eq. (50)

$$\Phi - \Phi_0 n = \Phi_0 f(K_s, K_d, \tilde{K}, \dots), \quad (51)$$

where n is the integer winding number and f is a function of the phenomenological parameters of the system, $|f| < 1$, for certain n . The flux in the domain boundary line depends on specific system properties and is not related in a simple way to an integer or rational multiple of Φ_0 . This flux line is a fractional vortex analogous to that found in Ref. 29.

On the other hand, the total flux to two neighboring domain boundary lines adds up to an integer multiple of Φ_0 , because in the integral on the right hand side of Eq. (50) the integrands are identical even in sign so that their contributions cancel,

$$\Phi_1 + \Phi_2 = n\Phi_0. \quad (52)$$

This has interesting consequences. A standard vortex trapped on a TB can decay into two fractional vortices, each with a flux smaller than Φ_0 , and gain magnetic line energy in this way. This decay pays only if the gain of field energy is not compensated by the energy expense to create two domain boundary lines. [Usually the field energy ($\propto \Phi^2$) is more important than the core energy in strongly type-II superconductors.] Fractional vortices cannot leave the TB, but are ‘‘pinned’’ on it. As a consequence flux flow parallel to the array of TB should be considerably easier than perpendicular to the TB.

Of course, an ideal experiment to verify the existence of fractional vortices on TB would be their direct observation by such tools as scanning SQUID microscopes, Hall probes, or electron holography, all of which allow a rather good measurement of the magnitude of local magnetic flux. Such experiments could be successful in rather weak magnetic fields where the vortices are rare and would almost exclusively reside on TB's due to the lower line energy or critical magnetic field. The observation of fractional vortices would be another indication for the correctness of our picture.

D. Soft mode

Finally we consider another indication of the occurrence of a new TB state at low temperatures. In connection with the transition of the TB state at T' a local softening of the mode of the relative phase θ is expected. In the TB state (II) fluctuations of the relative phase couple to the lattice strain $\epsilon = \epsilon_{xx} - \epsilon_{yy}$ as seen in Eqs. (8)–(10),

$$c \delta \epsilon (u \delta v + v \delta u) = c \delta \epsilon |\eta_s| |\eta_d| \sin \theta \delta \theta. \quad (53)$$

Due to this coupling the transition at T' would be accompanied by an anomaly in ultrasound absorption and a renormalization of the sound velocity for longitudinal sound waves along the main axis in a highly twinned sample. Such measurements could, however, be disturbed by scattering of ultrasound at the TB's.

VII. CONCLUSIONS

Among the experiments probing the symmetry of the superconducting order parameter of YBCO the one observing a Josephson coupling along the c axis is the most puzzling one, often used as an argument against ‘‘ d -wave superconductivity.’’¹³ We have examined here the conditions of this experiment assuming that the basic order parameter of YBCO has d -wave symmetry. Obviously, the orthorhombic distortion ($\epsilon_{xx} - \epsilon_{yy}$) of the crystal lattice of YBCO plays an important part in the Josephson coupling because there is no symmetry which would forbid it. While for a single-domain orthorhombic system the situation is rather simple, a more careful consideration is necessary for twinned samples. Our analysis shows that in the case of highly twinned sample still a sizable Josephson coupling is possible. We demonstrated that twin boundaries can provide a channel of coupling if they support a locally \mathcal{T} -violating state in their vicinity, while the twin domains contribute little due to destructive interference effect in the phase coherent tunneling. Although the coupling is very inhomogeneous in magnetitude and phase, we have seen that the properties of the junction on a macroscopic scale may look rather homogeneous.

In the Introduction we mentioned the measurement of the $I_c R$ product which is lower than one would expect from the theory by Ambegaokar and Baratoff.¹⁴ One source of the discrepancy between the calculated and the measured value lies in the assumption about the correct gap values for YBCO using the formula

$$I_c R = \frac{2}{e} \frac{\Delta_{\text{Pb}} \Delta_{\text{Y}}}{\Delta_{\text{Pb}} + \Delta_{\text{Y}}} K \left[\left| \frac{\Delta_{\text{Pb}} - \Delta_{\text{Y}}}{\Delta_{\text{Pb}} + \Delta_{\text{Y}}} \right| \right], \quad (54)$$

where Δ_{Pb} and Δ_{Y} are the measured gap values in Pb and YBCO, respectively, and K the complete elliptic integral.^{13,14} If we insert $\Delta_{\text{Pb}} = 1.4$ meV and $\Delta_{\text{Y}} = 14$ meV, then we obtain $I_c R \approx 5$ mV. However, the assumed gap value for YBCO corresponds to the one of the d -wave order parameter rather than to that of the induced s -wave component which actually is responsible for the Josephson coupling. For untwinned samples the measured $I_c R$ product lies between 1 and 2 mV which leads to a gap value of $\Delta_{\text{Y}} \sim 0.4$ –1 meV in Eq. (54), which may not be unreasonable for the induced s -wave order parameter. The reduction of the $I_c R$ product for twinned samples follows, of course, from the destructive interference effects and the fact that the dominant channel of coupling is provided by the \mathcal{T} -violating TB states. In this case no simple relation as in Eq. (54) is available. Naively, we would expect $I_c R$ to increase more or less proportionally with the density of TB's. However, as mentioned earlier, we should be cautious because the s -wave order parameter component would be suppressed if the average distance between TB's becomes comparable with its coherence length, as it is suppressed in the vicinity of the TB's. It is difficult to estimate this length and it might be considerably longer than the one of the d -wave order parameter [$\xi(T=0) \sim 10$ Å]. Consequently, it is difficult to predict the dependence of the $I_c R$ product on the density of TB's. Unfortunately, at present, there is no systematic experimental study on this problem.

The \mathcal{T} -violating twin boundary states correspond to a superconducting phase with local $s \pm id$ symmetry which is known to have no nodes in the gap. To ensure that this would

not spoil the experiments probing the density of states of the quasiparticles, one has to consider the quality of the samples used in these experiments. It turns out that samples used to measure the London penetration depth are rather weakly twinned with an average distance of $\sim 1 \mu\text{m}$ between twin boundaries. This leaves a lot of space with the $s \pm d$ bulk phase which has nodes in the gap.

We mentioned also that the virtual absence of Josephson coupling in BSCCO may originate from the different type of the orthorhombic distortion with a shear strain of the form ϵ_{xy} . In contrast to the case of YBCO there is no admixture of an s -wave component to the $d_{x^2-y^2}$ order parameter enforced by symmetry. The absence or rather small magnitude of such an s -wave component may explain the negative result found for c -axis Josephson coupling between BSCCO and a conventional s -wave superconductor.¹⁶ On the other hand, Kuboki and Lee²⁶ argued recently that an interlayer s -wave component is present in this system. This s -wave component itself, however, gives only a negligible contribution to the c -axis Josephson effect.²⁶ Instead it could induce orthorhombic distortion $\epsilon_{xx} - \epsilon_{yy}$, leading to a situation as in YBCO. However, since this distortion has not been detected so far, it is not possible to draw any firm conclusion on how interlayer pairing might affect the c -axis tunneling.

Finally, we like to mention that the interface with phase modulation θ could be an object for various new studies on pinning effects if d and λ_J are comparable. It will be interesting to analyze the static screening properties of the junction as well as the dynamics of φ and the current under this condition. This issue will be considered in a future publication.

ACKNOWLEDGMENTS

We are grateful to R.C. Dynes and A. Furusaki for stimulating discussions. We thank to the Swiss Nationalfonds (M.S.) and the Ministry of Education, Science and Culture of Japan (K.K.) for financial support. This work at MIT was supported primarily by NSF-MRSEC Grant No. DMR-94-00334.

APPENDIX A: INSTABILITY CONDITION OF THE TB STATE

In Sec. III we considered the instability of the TB state (I) analyzed by means of the linearized GL equation [Eq. (10)] of the imaginary parts u and v of the order parameters η_s and η_d . Here we give a solution of a simplified version of these equations. We assume that the length scale ξ of variation of η_s at the TB is very small compared with the one introduced by u and v ($\tilde{\xi}$). Therefore we replace $V(\tilde{x})$ by $\eta_{s0}^2 \xi \delta(\tilde{x} - \tilde{x}_0)$ and $Q(\tilde{x})$ by $Q_0 \text{sgn}(\tilde{x})$ in Eq. (10) (TB's located at \tilde{x}_0). We assume that $v(\tilde{x})$ is even and $u(\tilde{x})$ is odd [$u(\tilde{x}_0) = 0$]. We replace $u(\tilde{x})$ by $w(\tilde{x}) = u(\tilde{x}) \text{sgn}(\tilde{x})$ and Fourier transform the equations to obtain

$$(k^2 K_d + R_{d0}) \tilde{w}_k + Q_0 \tilde{v}_k = 0, \quad (\text{A1})$$

$$Q_0 \tilde{w}_k + (k^2 K_s + R_{s0}) \tilde{v}_k = 2b_s \eta_{s0}^2 \xi v(\tilde{x}_0) e^{ik\tilde{x}_0},$$

with

$$(v(\tilde{x}), w(\tilde{x})) = \frac{1}{2\pi} \int_{-\infty}^{+\infty} dk e^{-ik\tilde{x}} (\tilde{v}_k, \tilde{w}_k). \quad (\text{A2})$$

Note that the term $u(\tilde{x}) \delta(\tilde{x} - \tilde{x}_0)$ vanishes in the real space equation because of $u(\tilde{x}_0) = 0$. This set of equations can be solved at once and by Fourier transformation lead to

$$v(\tilde{x}) = \frac{v(\tilde{x}_0) \eta_{s0}^2 b_s \xi}{K_s K_d} \sum_{l=1,2} R(ik_l) e^{-k_l |\tilde{x} - \tilde{x}_0|}, \quad (\text{A3})$$

$$u(\tilde{x}) = \frac{v(\tilde{x}_0) \eta_{s0}^2 b_s \xi}{K_s K_d} \text{sgn}(\tilde{x}) \sum_{l=1,2} S(ik_l) e^{-k_l |\tilde{x} - \tilde{x}_0|}.$$

The functions R and S are obtained in the residuum calculation,

$$R(k) = \frac{i(k^2 K_d + R_{d0})}{k(2k^2 + r)} \quad \text{and} \quad S(k) = \frac{iQ_0}{k(2k^2 + r)}, \quad (\text{A4})$$

with $r = R_{s0}/K_s + R_{d0}/K_d$. The arguments $ik_{1,2}$ are the imaginary poles of \tilde{v}_k and \tilde{w}_k in the upper complex plane of k . We implicitly assumed here that $r^2 - 4q^2 > 0$ to ensure that these poles are purely imaginary [$q^2 = (R_{s0}R_{d0} - Q_0^2)/K_s K_d > 0$],

$$k_{1,2}^2 = r \pm \sqrt{r^2 - 4q^2}. \quad (\text{A5})$$

The smaller among the two, $k_1 = \tilde{\xi}^{-1}$, defines the longer length scale of v and u . In particular, note that $k_1 \rightarrow 0$ for $q \rightarrow 0$ which is the instability condition for the \mathcal{S} -violating bulk transition at $T^*(c\epsilon)$.

The instability condition for state (II) is obtained via the self-consistency equation for $v(\tilde{x}_0)$ which for $v(\tilde{x}_0) \neq 0$ leads to

$$1 = \frac{\eta_{s0}^2 b_s \xi}{K_s K_d} \sum_{l=1,2} R(ik_l). \quad (\text{A6})$$

The right hand side of this equation is smaller than 1 close to the onset of superconductivity, and hence for all $T > T'$, the instability temperature. Because $R(ik_1 \rightarrow 0) \rightarrow \infty$, we can conclude that $T' \geq T^*$ always.

We can easily extend our discussion to the case of two TB's located at \tilde{x}_0 and \tilde{x}_1 . Equation (A1) is modified by replacing the right hand side of the second equation by

$$2b_s \eta_{s0} \xi [v(\tilde{x}_0) e^{ik\tilde{x}_0} + v(\tilde{x}_1) e^{ik\tilde{x}_1}] \quad (\text{A7})$$

and adjusting also $Q(\tilde{x})$ appropriately. By symmetry there are only two possible candidates for the instability characterized by $v(\tilde{x}_1) = +v(\tilde{x}_0)$ (bonding) and $v(\tilde{x}_1) = -v(\tilde{x}_0)$ (antibonding). The self-consistence equation has then the form

$$1 = \frac{\eta_{s0}^2 b_s \xi}{K_s K_d} \sum_{l=1,2} R(ik_l) [1 \pm e^{-k_l |\tilde{x}_0 - \tilde{x}_1|}] \quad (\text{A8})$$

for the bonding (+) and antibonding (−) configuration. The bonding state leads to the first instability and has the higher transition temperature than the one of antibonding state, because the + sign increases the right hand side in the self-

consistence equation. Note that also for an entire whole array of TB's the symmetric configuration yields the preferred TB state.

Consequently, the relative phase θ varies only between 0 and π and passes through $\pi/2$ at each TB. For the antibonding state θ would pass at one TB through $\pi/2$ and at the next through $3\pi/2$ such that after passing through two TB's θ would have changed by 2π . However, this behavior is not favored energetically.

Let us briefly discuss two limiting cases. For very small orthorhombic distortion $c\epsilon$ the s -wave component of the order parameter is small, $\eta_{s0} \propto c\epsilon$. In order to satisfy the self-consistence equation $R(ik_j)$ has to become large. This is the case if $q \rightarrow 0$. Hence, for $c\epsilon \rightarrow 0$ the phase transition line $T'(c\epsilon)$ approaches gradually $T^*(c\epsilon)$. Finally we would like to demonstrate a scaling behavior to the self-consistence equation for very large values of $c\epsilon$. In this case the bulk values η_{s0} and η_{d0} have about the same magnitude and are proportional to $c\epsilon$. By redefining the temperature as $\hat{T}c\epsilon = T$ and the unit length as $\hat{x}/\sqrt{c\epsilon} = \tilde{x}$, we observe that up to a correction of the order $a_d/c\epsilon$ the right hand side of Eq. (A6) does not depend on $c\epsilon$. Therefore we find that the instability temperature T' is proportional to $c\epsilon$ and the ratio of $T'(c\epsilon)/T_c(c\epsilon)$ approaches a constant for large $c\epsilon$ as shown in the example of Fig. 4.

APPENDIX B: THE JUNCTION IN A MAGNETIC FIELD

We analyze here the properties of the junction in a field in more detail in order to demonstrate the validity of the expressions given in Sec. V.

1. Fraunhofer pattern

We consider again the limit $N \gg 1$. With an external magnetic field parallel to the TB the local Josephson current has the form

$$J(\tilde{x}) = I_c(\tilde{x}) \sin[\varphi + k\tilde{x} - \theta(\tilde{x})], \quad (\text{B1})$$

where $k = 2\pi B\tilde{d}/\Phi_0$ where in the small field limit $kd \ll 1$. In order to calculate the total current in the region $-L/2 \leq \tilde{x}, \tilde{y} \leq L/2$ ($L = Nd$), we perform the \tilde{y} integration immediately and divide the remaining \tilde{x} integral into two parts,

$$I_{(1)} = L \sum_{n=0}^{N-1} \cos(\varphi + k\tilde{x}_n) \int_{\tilde{x}_n - \tilde{\xi}}^{\tilde{x}_n + \tilde{\xi}} d\tilde{x} I_c(\tilde{x}) \sin[k(\tilde{x} - \tilde{x}_n) - \theta(\tilde{x})] \approx (I_c \sin\theta) L d \sum_{n=0}^{N-1} \cos(\varphi + k\tilde{x}_n) \quad (\text{B2})$$

and

$$I_{(2)} = L \sum_{n=0}^{N-1} \sin(\varphi + k\tilde{x}_n) \int_{\tilde{x}_n - \tilde{\xi}}^{\tilde{x}_n + \tilde{\xi}} d\tilde{x} I_c(\tilde{x}) \cos[k(\tilde{x} - \tilde{x}_n) - \theta(\tilde{x})] \approx L \sum_{n=0}^{N-1} \sin(\varphi + k\tilde{x}_n) (-1)^n \left[I_{c2}(\tilde{x}_{n+1} - \tilde{x}_n - 2\tilde{x}') - \frac{2\tilde{\xi} I_{c1}}{\pi} \cos\left(\frac{\pi\tilde{x}'}{2\tilde{\xi}}\right) \right], \quad (\text{B3})$$

where we used that $kd, k\tilde{\xi} \ll 1$. First, we consider $I_{(1)}$ by rewriting this expression into a form where we easily perform the average of the ζ_n and the summation over n ,

$$I_{(1)} = \langle I_c \sin\theta \rangle L d \operatorname{Re} \left\{ e^{i\varphi} \sum_{n=0}^{N-1} \exp \left[ik \left(dn + \sum_{j=0}^n \zeta_j \right) \right] \right\} = \langle I_c \sin\theta \rangle L d \operatorname{Re} \left[e^{i\varphi} \frac{1 - g^N e^{ikL}}{1 - g e^{ikd}} \right], \quad (\text{B4})$$

where we averaged by using $\langle e^{ik\zeta} \rangle = e^{-k^2 \langle \zeta^2 \rangle / 2} = e^{-k^2 \sigma^2 / 2} = g$. In the small field limit various approximations are allowed now: $g \approx 1 + O((k\sigma)^2)$, $1 - g^N = (b\sigma/2) b\sigma N = O(k\sigma)$, and $\cos(\alpha + kd) = \cos(\alpha) + O(kd)$. This leads to the following final expression for $I_{(1)}$:

$$I_{(1)} = \langle I_c \sin\theta \rangle L^2 \frac{\sin(kL/2)}{kL/2} \cos(\varphi + kL/2) + O(kd). \quad (\text{B5})$$

We turn now to $I_{(2)}$. As neighboring domains tend to cancel each other we combine them and make use of the central limit theorem which leads to the following sum whose imaginary part apart from prefactors will be relevant for us:

$$\begin{aligned} & \left\langle \sum_{n=0}^{N/2-1} e^{i(\varphi + k\tilde{x}_{2n})} (\zeta_{2n+1} - \zeta_{2n+2}) \right\rangle \\ &= \left[\left\langle \left\{ \sum_{n=0}^{N/2-1} e^{i(\varphi + k\tilde{x}_{2n})} (\zeta_{2n+1} - \zeta_{2n+2}) \right\}^2 \right\rangle \right]^{1/2} \\ &= \left[2\sigma^2 e^{2i\varphi} \sum_{n=0}^{N/2-1} g^{8n} e^{4inkd} \right]^{1/2} \\ &= \sigma e^{i(\varphi - kL/2)} \sqrt{\frac{\sin(kL)}{\sin(kd)}} + O(kd). \end{aligned} \quad (\text{B6})$$

Using the results from Sec. IV this can be translated easily into the expression

$$I_{(2)} = \langle I_c \cos\theta \rangle L^2 \sqrt{\frac{\sin(kL)}{kL}} \sin(\varphi + bL/2) + O(bd). \quad (\text{B7})$$

Therefore the total current is given by $I = I_{(1)} + I_{(2)}$ and the maximal current which can pass through the junction is

$$I_{\max} = L^2 \left\{ \left[\langle I_c \sin\theta \rangle F\left(\frac{\pi\Phi}{\Phi_0}\right) \right]^2 + \langle I_c \cos\theta \rangle^2 F\left(\frac{2\pi\Phi}{\Phi_0}\right) \right\}^{1/2} \quad (\text{B8})$$

[$F(x) = \sin(x)/x$], which in the large- N limit is dominated by the first term

$$I_{\max} = \langle I_c \sin\theta \rangle L^2 \left| F\left(\frac{\pi\Phi}{\Phi_0}\right) \right| + O(N^{-1}). \quad (\text{B9})$$

This corresponds to the standard interference pattern and is equivalent to the expression given in Sec. V for the large- N limit.

2. Phase modulation

As we mentioned in Sec. V, $\theta(\tilde{x})$ imposes a modulation of the Josephson current phase relation. We show here that this modulation is not harmful for the Fiske resonance (as well as the Fraunhofer pattern). For this purpose we analyze here the Fourier decomposition of the phase modulation

$$I_c(\tilde{x})e^{-i\theta(\tilde{x})} = \sum_{n=0}^{\infty} h_n e^{-iq_n\tilde{x}}, \quad (\text{B10})$$

where, due to the finite extension ($L \times L$) of the interface, the wave vector q is discrete, $q_n = 2\pi n/dN = 2\pi n/L$. (We assume again that the TB's are parallel to the edges of the square.) It is straightforward to calculate h_n as

$$h_n = \frac{1}{L} \int_0^L d\tilde{x} I_c(\tilde{x}) e^{-i\theta(\tilde{x})} e^{iq_n\tilde{x}} = \langle I_c(\tilde{x}) e^{-i\theta(\tilde{x})} e^{iq_n\tilde{x}} \rangle, \quad (\text{B11})$$

We are allowed to use the average over the ζ when N is very large. Hence, the component of $n=0$ is nothing but the average used in Secs. IV and V,

$$h_0 = \langle I_c e^{-i\theta} \rangle. \quad (\text{B12})$$

For the expressions of $n > 0$ we restrict ourselves to the limit $d \gg \tilde{\xi}$,

$$h_n = \frac{i}{L} \frac{1 - e^{-q_n^2 \sigma^2 N/2}}{1 - e^{i2q_n d - q_n^2 \sigma^2}} (h_n^{(1)} + h_n^{(2)}), \quad (\text{B13})$$

with

$$h_n^{(1)} = 2\tilde{\xi} I_{c1} \cos(q_n \tilde{\xi}) \left\{ \frac{1}{2q_n \tilde{\xi} - \pi} - \frac{e^{iq_n d - q_n^2 \sigma^2/2}}{2q_n \tilde{\xi} + \pi} \right\}, \quad (\text{B14})$$

$$h_n^{(2)} = \frac{2I_{c2}}{q_n} e^{iq_n d - q_n^2 \sigma^2/2} \left\{ \cos(q_n \tilde{\xi}) - \cos\left(q_n(d - \tilde{\xi}) + i \frac{q_n^2 \sigma^2}{2}\right) \right\}.$$

For $n \sim mN/2$, h_n has peaks more or less pronounced depending on the ratio σ/d (m is an integer). If $\sigma/d \ll 1$ (the TB's form an almost regular lattice),

$$\left| \frac{h_{N/2}}{h_0} \right| \sim \frac{\alpha}{N} \frac{q_{N/2}^2 \sigma^2 N/2}{q_{N/2}^2 \sigma^2} \sim \alpha/2, \quad (\text{B15})$$

where α is of order 1. For a more realistic ratio of $\sigma/d \sim 0.1$, however,

$$\left| \frac{h_{N/2}}{h_0} \right| \sim \frac{\alpha'}{N} \frac{1}{1 - e^{-(\pi\sigma/d)^2}} \sim \frac{\alpha' d^2}{N\pi\sigma^2}, \quad (\text{B16})$$

with α' of order 1. Thus $|h_{N/2}|$ is strongly reduced compared with $|h_0|$ and it is easy to see that $|h_{mN/2}| < |h_{N/2}|$ for $m > 1$.

Note also that $|h_n/h_0| \sim 2\pi n \sigma^2/d^2 N$ for $n \ll N$. Therefore we can assume that h_0 represents by far the largest contribution in Eq. (B12).

We now turn to the problem of the Fiske resonances where the phase $\tilde{\varphi}$ of Eq. (36) is given more generally now by the superposition

$$\tilde{\varphi}(\tilde{x}, t) = \frac{2\pi\tilde{d}}{\Phi_0} \sum_n \text{Im} \left(\frac{h_n e^{i[\omega t - (k+q_n)\tilde{x} + \alpha]}}{\omega^2/v^2 - (k+q_n)^2 - i\Gamma\omega} \right). \quad (\text{B17})$$

Because $\tilde{\varphi}$ is small, we find for the dc current

$$\begin{aligned} J_{\text{dc}} &= \lim_{T \rightarrow \infty} \int_0^T dt \int_0^L d\tilde{x} \frac{1}{T} \text{Im} \sum_n h_n e^{i[\omega t - (k+q_n)\tilde{x} + \alpha + \tilde{\varphi}(\tilde{x}, t)]} \\ &= \frac{\pi\tilde{d}}{\Phi_0} \int_0^L d\tilde{x} \sum_{n, n'} \frac{h_n h_{n'}^* \Gamma \omega \cos[(q_n - q_{n'})\tilde{x}]}{[\omega^2/v^2 - (k+q_{n'})^2] + \Gamma^2 \omega^2} \\ &= \frac{\pi\tilde{d}}{\Phi_0} \sum_n \frac{|h_n|^2 \Gamma \omega}{[\omega^2/v^2 - (k+q_n)^2]^2 + \Gamma^2 \omega^2}, \end{aligned} \quad (\text{B18})$$

where the largest contribution originates from the $n=0$ term which is identical to Eq. (32). All other terms are diminished by a factor of the order N^{-2} , apart from $n \sim N/2, N, \dots$, which are of order $N^{-2}(d/\sigma)^4$. In principle, such terms could lead to small resonances at rather high magnetic fields, in particular, for $k \sim \pi m/d$. Only such high fields could produce a clear sign of the inhomogeneous nature of the Josephson coupling.

*Permanent address: Theoretische Physik, ETH-Hönggerberg, 8093 Zürich, Switzerland.

†Permanent address: Department of Physics, Kobe University, Kobe 657, Japan.

¹B.G. Levi, Phys. Today **46**(5), 17 (1993); R.C. Dynes, Solid State Commun. **92**, 53 (1994); J.R. Schrieffer, *ibid.* **92**, 129 (1994).

²W.N. Hardy, D.A. Bonn, D.C. Morgan, R. Liang, and K. Zhang, Phys. Rev. Lett. **70**, 3999 (1993).

³Z.X. Shen, D.S. Dessau, B.O. Wells, D.M. King, W.E. Spicer, A.J. Arko, D. Marshall, L.W. Lombardo, A. Kapitulnik, P. Dickinson, S. Doniach, J. DiCarlo, A.G. Loeser, and C.H. Park, Phys. Rev. Lett. **70**, 1553 (1993).

⁴H. Ding, J.C. Campuzano, A.F. Bellman, T. Yokoyama, M.R. Norman, M. Randeria, T. Takahashi, H. Katayama-Yoshida, K. Kadowaki,

and G. Jennings, Phys. Rev. Lett. **74**, 2784 (1995).

⁵P. Svedlindh, K. Niskanen, P. Norling, P. Nordblad, L. Lundgren, B. Lönnberg, and T. Lundström, Physica C **162-164**, 1365 (1989); W. Braunisch, N. Knauf, V. Kataev, S. Neuhäuser, A. Grütz, A. Kock, B. Roden, D. Khomskii, and D. Wohlleben, Phys. Rev. Lett. **68**, 1908 (1992).

⁶M. Sigrist and T.M. Rice, J. Phys. Soc. Jpn. **61**, 4283 (1992); J. Low Temp. Phys. **95**, 389 (1994).

⁷D.A. Wollman, D.J. Van Harlingen, W.C. Lee, D.M. Ginsberg, and A.J. Leggett, Phys. Rev. Lett. **71**, 2134 (1993); D. Brawner and H.R. Ott, Phys. Rev. B **50**, 6530 (1994); A. Mathai, Y. Gim, R.C. Black, A. Amar, and F.C. Wellstood, Phys. Rev. Lett. **74**, 4523 (1995).

⁸C.C. Tsuei, J.R. Kirtley, C.C. Chi, L.S. Yu-Jahnes, A. Gupta, T.

- Shaw, J.Z. Sun, and M.B. Ketchen, Phys. Rev. Lett. **73**, 593 (1994); J.R. Kirtley, C.C. Tsuei, J.Z. Sun, C.C. Chi, L.S. Yu-Jahnes, A. Gupta, M. Rupp, and M.B. Ketchen, Nature **373**, 225 (1995).
- ⁹I. Iguchi and Z. Wen, Phys. Rev. B **49**, 12388 (1994); D.A. Wollman, D.J. Van Harlingen, J. Giapintzakis, and D.M. Ginsberg, Phys. Rev. Lett. **74**, 797 (1995).
- ¹⁰P. Chaudhari and S.Y. Lin, Phys. Rev. Lett. **72**, 1048 (1994).
- ¹¹A.J. Millis, Phys. Rev. B **49**, 15408 (1994).
- ¹²J.R. Kirtley, P. Chaudhari, M.B. Ketchen, N. Khare, S.-Y. Lin, and T. Shaw, Phys. Rev. B **51**, 12057 (1995).
- ¹³A.G. Sun, D.A. Gajewski, M.B. Maple, and R.C. Dynes, Phys. Rev. Lett. **72**, 2267 (1994); A.S. Katz, A.G. Sun, R.C. Dynes, and K. Char, Appl. Phys. Lett. **66**, 105 (1995).
- ¹⁴V. Ambegaokar and A. Baratoff, Phys. Rev. Lett. **10**, 486 (1963).
- ¹⁵S.K. Yip, O.F. De Alcantara Bonfim, and P. Kumar, Phys. Rev. B **41**, 11214 (1990).
- ¹⁶H.Z. Durusoy, D. Lew, L. Lombardo, A. Kapitulnik, T.H. Geballe, and M.R. Beasley (unpublished).
- ¹⁷For a review see M. Sigrist and K. Ueda, Rev. Mod. Phys. **63**, 239 (1991).
- ¹⁸J. Betonras and R. Joynt (unpublished).
- ¹⁹H. You, U. Welp, and Y. Fang, Phys. Rev. B **43**, 3660 (1991).
- ²⁰A.J. Millis and K.M. Rabe, Phys. Rev. B **38**, 8908 (1988).
- ²¹A.J. Leggett (private communication).
- ²²M.B. Walker (unpublished).
- ²³The most stable twin boundary state should satisfy the constraint that the current perpendicular to the twin boundary be zero, $J_{\tilde{x}} = (4\pi c/\Phi_0)\{K_s(\eta_{s1}\eta'_{s2} - \eta_{s2}\eta'_{s1}) + K_d(\eta_{d1}\eta'_{d2} - \eta_{d2}\eta'_{d1})\}$ ($\eta_{\mu} = \eta_{\mu 1} + i\eta_{\mu 2}$, $\mu = s, d$), where the prime denotes the derivative with respect to \tilde{x} . This condition is violated because we neglected the vector potential \mathbf{A} , which would introduce the necessary corrections $-(8\pi^2 c/\Phi_0)A_{\tilde{x}}(K_s|\eta_s|^2 + K_d|\eta_d|^2)$.
- ²⁴See, for example, M. Tinkham, *Introduction to Superconductivity* (McGraw-Hill, New York, 1975).
- ²⁵R.E. Eck, D.J. Scalapino, and B.N. Taylor, Phys. Rev. Lett. **13**, 15 (1964).
- ²⁶K. Kuboki and P.A. Lee, J. Phys. Soc. Jpn. (to be published); (unpublished).
- ²⁷The variation of $\theta(\tilde{x})$ causes the appearance of another length scale of φ . This is the length L_0 over which φ varies by about π taking advantage of the fluctuation of θ . Note that this length is analogous to that found in the context of pinning of charge density wave on random impurities [see H. Fukuyama and P.A. Lee, Phys. Rev. B **17**, 535 (1978); P.A. Lee and T.M. Rice, *ibid.* **19**, 3970 (1979)]. This length L_0 is easily estimated (in case $d \ll \xi$) to be $L_0 = (4\pi^2/3)^{2/3}\lambda_J(\lambda_J/d)^{1/3}(d/\sigma)^{2/3}$, which is larger than λ_J and in our case also larger than the linear extension L of the interface. Note that L_0 increases with growing ratio λ_J/d . In our discussion we need not to take L_0 into account. The “wandering” of φ is, however, an interesting phenomenon which is not found in ordinary Josephson junctions.
- ²⁸G.E. Volovik and L.P. Gor'kov, Zh. Éksp. Teor. Fiz. **88**, 1412 (1985) [Sov. Phys. JETP **61**, 843 (1985)].
- ²⁹M. Sigrist, N. Ogawa, and K. Ueda, J. Phys. Soc. Jpn. **60**, 2341 (1991).
- ³⁰M. Sigrist, T.M. Rice, and K. Ueda, Phys. Rev. Lett. **63**, 1727 (1989).